



UNIVERSITÀ POLITECNICA DELLE MARCHE
Repository ISTITUZIONALE

A methodology to forecast the main non-dimensional performance parameters of pumps-as-turbines (PaTs) operating at Best Efficiency Point (BEP)

This is the peer reviewed version of the following article:

Original

A methodology to forecast the main non-dimensional performance parameters of pumps-as-turbines (PaTs) operating at Best Efficiency Point (BEP) / Renzi, M., Nigro, A., Rossi, M.. - In: RENEWABLE ENERGY. - ISSN 0960-1481. - 160:(2020), pp. 16-25. [10.1016/j.renene.2020.05.165]

Availability:

This version is available at: 11566/288892 since: 2024-11-21T14:02:01Z

Publisher:

Published

DOI:10.1016/j.renene.2020.05.165

Terms of use:

The terms and conditions for the reuse of this version of the manuscript are specified in the publishing policy. The use of copyrighted works requires the consent of the rights' holder (author or publisher). Works made available under a Creative Commons license or a Publisher's custom-made license can be used according to the terms and conditions contained therein. See editor's website for further information and terms and conditions.

This item was downloaded from IRIS Università Politecnica delle Marche (<https://iris.univpm.it>). When citing, please refer to the published version.

(Article begins on next page)

A methodology to forecast the main non-dimensional performance parameters of Pumps-as-Turbines (PaTs) operating at Best Efficiency Point (BEP)

Massimiliano Renzi^{a,*}, Alessandra Nigro^a, Mosè Rossi^a

^a*Free University of Bozen-Bolzano, Faculty of Science and Technology, Piazza Università 5, 39100, Bolzano, Italy*

Abstract

This work presents a model based on analytical equations to identify the Best Efficiency Point (BEP) of Pumps-as-Turbines (PaTs). The equations are developed exploiting an experimental data-set of 59 PaTs, obtained in both pump and turbine modes, in form of non-dimensional parameters. Data analysis shows a linear correlation between specific speeds in pump and turbine modes, as well as between specific diameters in both operating modes. An additional indicator of the PaT performance, which is often disregarded in literature works, is presented: a second order polynomial equation to forecast the mechanical efficiency of PaTs in turbine mode is developed using the values of specific speed and mechanical efficiency in pump mode as independent variables. Performance data obtained through experiments and numerical simulations of six PaTs, which were not used in the development of the model, are employed to validate and assess the accuracy of the proposed analytical equations. The prediction capability of the model is also compared to other four models available in literature. Results demonstrate a good forecast capability and a general better agreement with respect to experimental and numerical data. A further improvement of the model can be achieved by extending the experimental data-set with additional PaTs typologies.

Keywords: Pumps-as-Turbines, Best Efficiency Point, Prediction model, Non-dimensional analysis, Energy recovery

*Corresponding author

Email address: `massimiliano.renzi@unibz.it` (Massimiliano Renzi)

Nomenclature

Physics magnitudes

Q	Volumetric flow rate [m^3/s]
H	Head [m]
ρ	Density [kg/m^3]
g	Gravitational acceleration [m/s^2]
P	Mechanical power [W]
D	Impeller outer diameter [m]
ω	Rotating speed [rad/s]
Φ	Flow coefficient [-]
Ψ	Head coefficient [-]
η	Mechanical efficiency [-]
Λ	Power coefficient [-]
N_s	Specific speed [-]
D_s	Specific diameter [-]

Subscripts

p	Pump mode operation
t	Turbine mode operation
BEP	Best Efficiency Point
$Exp.$	Experimental
CFD	Computational Fluid Dynamics
$Model$	Presented prediction model

1. Introduction

Large-scale hydropower has experienced a reduction of both installations and economical investments in developed countries since the main available natural water sources have been exploited and new civil works required for these power plants would have a significant environmental impact. As a consequence, the hydropower sector is currently shifting from large-scale plants to small-scale ones [1, 2]. Besides the production of electricity in remote and rural zones, where the development of an electric grid is not easy [3], small-scale hydropower also includes energy recovery applications such as Water Distribution Networks (WDNs) [4, 5], wastewater plants [6] and irrigation systems [7, 8]. The technologies used in small-scale applications have the same operating principle of the large-scale ones, even though several important modifications on hydraulic machines are essential to obtain high performance in each single installation site.

Among them, Pumps-as-Turbines (PaTs) are dominating the field due to their cheaper cost and larger spare parts availability compared to traditional hydraulic turbines [9, 10]. Nevertheless, the evaluation of PaTs performance in off-design operating conditions, as well as the forecast of their Best Efficiency Point (BEP), is still an issue due to the small number of operating data used to develop most of the models available in literature [11, 12].

With regards to the performance prediction of Pumps-as-Turbines (PaTs), when dealing with off-design operating conditions, published work has only appeared recently. For instance, Huang et al. [13] proposed a theoretical approach to forecast both flow rate and head obtained when a PaT operates in pump or in turbine mode. The model is based on the characteristic matching between rotor and stator, but the knowledge of the main geometrical parameters of a PaT are required.

In order to bypass the need for the availability of the geometrical parameters, which are not easy to get from pump manufacturers, other studies proposed methodologies to forecast PaT performance from given design parameters in turbine mode. Delgado et al. [14] developed a new methodology with the aim of predicting the performance curves of a PaT and its rotational speed through a Hermite polynomial chaos expansion. This tool is intended to improve the management of the operation of PaTs in specific hydropower applications. Novara et al. [15] proposed a model, which is based on fixed-coefficient polynomials, to forecast the performance curves of a PaT from a given BEP. The model was validated through experimental data of some PaTs available in literature. Furthermore, the authors of this paper have proposed an analytical model that

38 was validated through experimental and numerical data related to three differ-
39 ent centrifugal PaTs [16] not included in the development of the model itself.
40 The model, which was presented in [16], relies on experimental data of 32 PaTs
41 [9, 17, 18, 19, 20, 21, 22, 23, 24, 25] and it is based on both non-dimensional anal-
42 ysis and a normalization process to predict the off-design performance of PaTs.
43 The model provides simple analytical equations that can be used in a range of
44 specific speeds between 0.09 and 2.24. However, also in this case, the knowledge
45 of the BEP flow rate and head coefficients, as well as the efficiency in turbine
46 mode, is needed a priori.

47 Several authors proposed analytical equations that correlate the main pump
48 data with those in turbine mode, to predict the BEP in turbine mode, since the
49 knowledge of pump data is easily available from pump manufacturers. Among
50 them, Alatorre-Frenk [26], Schmiedl [27] and Grover [28] developed analytical
51 methodologies aimed at evaluating flow rate, head and mechanical efficiency of
52 PaTs operating in turbine mode. However, their empirical correlations were ob-
53 tained using the experimental results of a single or a limited number of PaTs,
54 showing good prediction capabilities only for narrow ranges of specific speeds.

55 Recently, other predictive models were developed with the aim of forecast-
56 ing both BEP and off-design operating conditions. Barbarelli et al.[24] proposed
57 a one-dimensional code capable of reconstructing the performance curves of a
58 PaT, BEP included, using information related to the main geometrical character-
59 istics of pumps. The validation of the code was carried out from experimental
60 results of 12 different PaTs as reported in [29]. However, also this code requires
61 specific geometrical input parameters, which are not always available nor freely
62 provided by the manufacturers, thus resulting in a complex tool for predicting
63 the performance of a PaT. Some of the authors of this work also developed a
64 new model, based on Artificial Neural Networks (ANNs) capable of reconstruct-
65 ing off-design operating conditions of PaTs, including BEP values [30]. The data
66 used for training the networks refer to the same experimental values used in [16].
67 The predicted results were compared with the experimental ones obtained by a
68 centrifugal PaT that was not involved in the training process, showing a general
69 good agreement for both off-design operating points and for the BEP. Venturini
70 et al. [31] developed a physics-based simulation model able to forecast PaTs per-
71 formance curves over the entire operation range based on pump characteristics,
72 coupled with an optimization tool to define the main geometrical parameters of
73 the machine in case these design data are not available.

74 Regarding the prediction of the mechanical efficiency at BEP in turbine mode,
75 several prediction models suggest to use the same value obtained in pump mode

76 [32, 33]. However, this assumption might be a limitation because the mechanical
77 efficiency of a PaT at BEP can vary depending on the internal fluid dynamic be-
78 haviour of the flow and on the external operating conditions [16]. To the authors'
79 knowledge, only some works supplied a model for the evaluation of the mechan-
80 ical efficiency in turbine mode, such as the one of Tan et al. [25]. Alatorre-Frenk
81 [26] supplied an equation where the efficiency in pump mode is used. Schmiedl
82 [27] relates the efficiency in turbine mode to the one in pump mode, as well as to
83 the specific speed in turbine mode, while Grover [28] requires to input a priori
84 the specific speed value of a PaT in turbine mode.

85 The authors of this work used a large experimental data-set composed of 59
86 different BEP values in both pump and turbine modes, whose data were collected
87 in [16] and [34]. This large data-set allowed the range of validity of the model to
88 be widened and the performance prediction accuracy. Therefore, the final aim of
89 this work is to provide a new set of equations, which are developed to identify
90 the BEP of PaTs, able to predict flow and head coefficients, as well as the me-
91 chanical efficiency at BEP, with a high accuracy and with a better generalization
92 capability, using only the main design data of the pump mode operation. After a
93 non-dimensional analysis of the used data-set, two correlations are proposed to
94 forecast the specific speed and the specific diameter of the PaT at BEP in turbine
95 mode, knowing the corresponding values in pump mode. Once these two val-
96 ues are known, both flow and head coefficients are evaluated using well-known
97 formulations for turbomachines and, subsequently, their dimensional values are
98 computed. Moreover, a new correlation for the prediction of the mechanical ef-
99 ficiency at BEP in turbine mode is supplied by linking two parameters at BEP in
100 pump mode, namely the specific speed and the mechanical efficiency.

101 The present paper is structured as follows: Section 2 describes i) the experi-
102 mental data-set and its elaboration using the non-dimensional analysis and ii) the
103 mathematical formulas used for the prediction of the main magnitudes of the
104 PaTs at BEP in turbine mode. Section 3 resumes the description of both the
105 experimental apparatus and the Computational Fluid Dynamics (CFD) models
106 employed to obtain experimental and numerical data of six different PaTs stud-
107 ied by the authors of this work and by other scientists, whose some of them
108 were provided by the Brno University of Technology (BUT) and the Polytech-
109 nic University of Bari (POLIBA). Subsequently, these data were used in Section
110 4 to validate the proposed model that is finally compared with those available
111 in literature, such as [25, 26, 27, 28], in order to evaluate and assess its accuracy.
112 Finally, Section 5 reports the conclusions of the work.

113 **2. Research and methods**

114 *2.1. Experimental data-set and non-dimensional analysis*

115 Experimental data of 59 PaTs operating at BEP in both pump and turbine
 116 modes were collected from the literature and rearranged by means of the non-
 117 dimensional analysis.

118 These data were used in the proposed prediction model in order to provide
 119 correlations between the operating modes of PaTs. Specifically, the formulations
 120 aim to predict specific speed, specific diameter and mechanical efficiency of PaTs,
 121 operating in turbine mode, using the same parameters in pump mode as input
 122 values. The hydraulic machines involved in this work are included in a wide
 123 range of operating conditions and dimensions as listed in in Table 1. Most of
 124 them belong to the categories of radial and mixed-flow hydraulic machines.

125 Figure 1 shows the distribution of the 59 BEP values in terms of flow rate vs
 126 head (left) and flow rate vs efficiency (right), showing that the majority of data
 127 are within the range of flow rate $0.00 [m^3/s] - 0.10 [m^3/s]$.

Table 1: Range of BEP values related to 59 PaTs operating in pump mode

Flow rate	Head	Rotating speed	Impeller diameter	Specific speed	Mechanical efficiency
$[m^3/s]$	$[m]$	$[rpm]$	$[m]$	$[-]$	$[-]$
$[0.005 - 0.222]$	$[4.00 - 135.00]$	$[750 - 2445]$	$[0.139 - 0.330]$	$[0.09 - 2.24]$	$[0.44 - 0.87]$

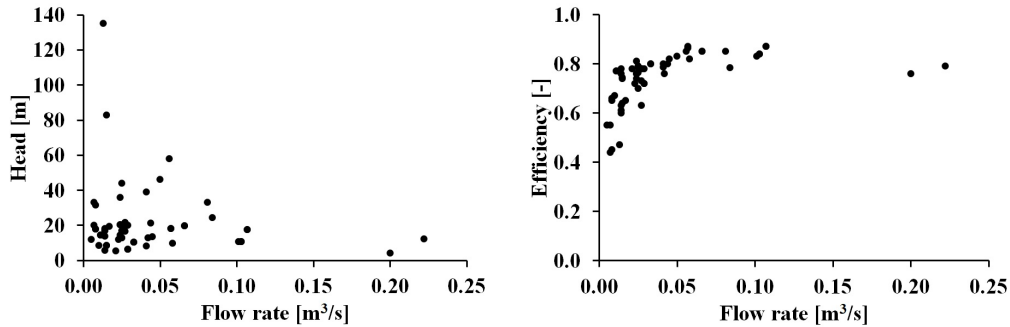


Figure 1: Flow rate vs head (left) and flow rate vs efficiency (right) of 59 PaTs operating in pump mode

The non-dimensional analysis of the experimental data-set, commonly used for extending operating data to other hydraulic machines that operate with the

same fluid dynamic similarity conditions, involves the evaluation of the flow coefficient (Φ) and the head coefficient (Ψ). Knowing the values of both flow and head coefficients, the specific speed (N_s) and the specific diameter (D_s) are obtained by means of Equations (1) and (2), respectively:

$$N_s = \frac{\sqrt{\Phi}}{\sqrt[4]{\Psi^3}}, \quad (1)$$

$$D_s = \frac{\sqrt[4]{\Psi}}{\sqrt{\Phi}}, \quad (2)$$

128 Both N_s and D_s are mainly used for classifying the hydraulic machines ac-
 129 cording to their design and, subsequently, their fluid path (e.g. radial, mixed-flow
 130 and axial).

131 2.2. Methodology used to predict PaTs performance at BEP

Both N_s and D_s parameters, which were evaluated by means of the experi-
 mental data-set related to 59 PaTs operating in both pump (p) and turbine modes
 (t), were used to develop the following functions:

$$N_{st} = f(N_{sp}), \quad D_{st} = f(D_{sp}). \quad (3)$$

132 The first function is expressed by Equation (4), which expresses N_{St} as a
 133 function of N_{Sp} :

$$N_{st} = 0.9051 \cdot N_{sp}. \quad (4)$$

134 This is a first order equation that fits accurately the collected experimental
 135 data-set, achieving an R^2 -value equal to 0.9488. It is worth noticing that an
 136 increase to a second order would have led to a minimal improvement (+1.6%)
 137 in terms of R^2 -value with respect to Equation (4); for this reason, a first order
 138 equation was chosen. Such a result allows us to conclude that there is a good
 139 correlation between the specific speed in pump and in turbine modes considering
 140 the investigated hydraulic machines and operating ranges of non-dimensional
 141 parameters. Figure 2 shows the correlation expressed by Equation (4) together
 142 with the experimental points available in the data-set (black dots).

143 Similarly, the second function is reported in Equation (5), which expresses
 144 D_{St} as a function of D_{Sp} :

$$D_{st} = 0.9436 \cdot D_{sp}. \quad (5)$$

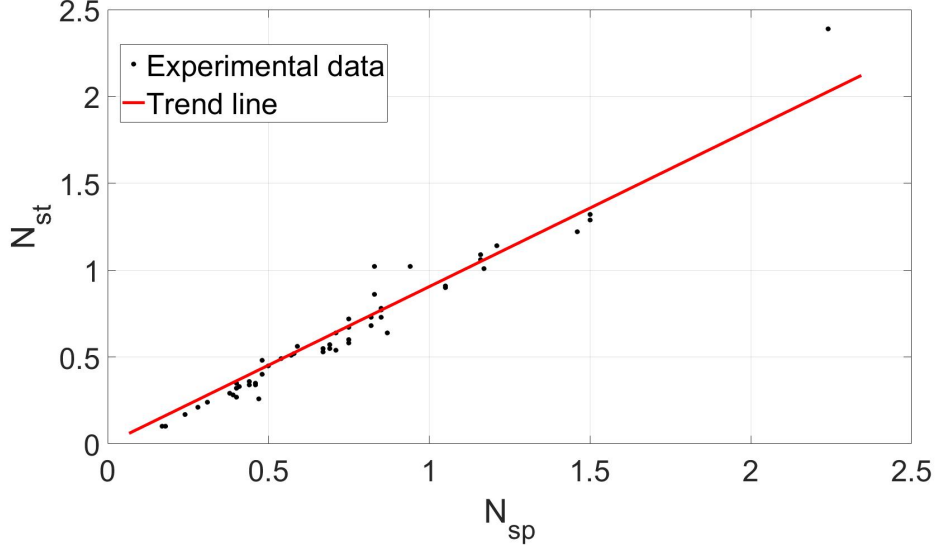


Figure 2: Correlation between N_{sp} and N_{st} values at respective BEPs

145 This is a first order equation that fits accurately the collected experimental
 146 data-set, achieving an R^2 -value equal to 0.986. Also in this case, since the lin-
 147 ear equation fits accurately the experimental values, an increase of the equation
 148 order would have led to a minor improvement of the R^2 -value (+0.2%) with
 149 respect to Equation (5); thus, a linear equation was chosen. Figure 3 displays
 150 the correlation expressed by Equation (5) together with the experimental points
 151 available in the data-set (black dots). The trend line in Figure 3 shows a similar
 152 behaviour as the one in Figure 2. It is worth noticing that the majority of the
 153 points that are shown in Figures 2 and 3 refer to radial and mixed-flow hydraulic
 154 machines. For this reason, it is suggested to apply the proposed model only for
 155 PaTs having an N_{sp} lower than 1.5, as well as a D_{sp} lower than 10. As previously
 156 mentioned in Section 1, also Tan et al. [25] proposed linear correlations between
 157 N_{sp} and N_{st} , as well as between D_{sp} and D_{st} , obtaining different coefficients.
 158 However, the number of data used by [25] was lower than the one reported in
 159 this work since only four PaTs were employed to develop the correlations, thus
 160 resulting in a narrow range of both N_s [0.58 – 1.52] and D_s [1.24 – 2.80].

161 Knowing the data of N_{sp} and D_{sp} at BEP of a generic pump, both N_{st} and D_{st}
 162 at BEP in turbine mode are evaluated by means of Equations (4) and (5). Once
 163 N_{st} and D_{st} are predicted, the values of Φ_t and Ψ_t are calculated by solving the

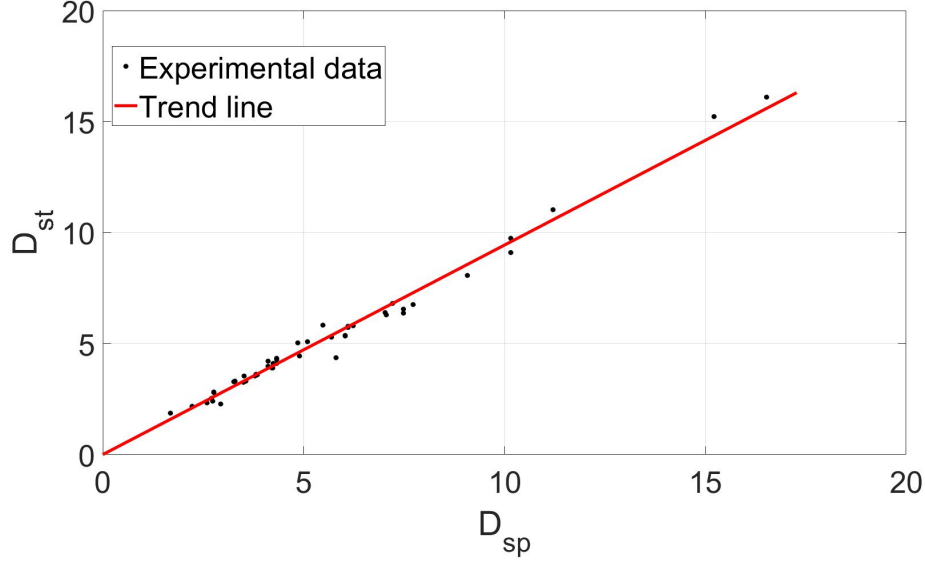


Figure 3: Correlation between D_{sp} and D_{st} values at respective BEPs

164 following two-equation system:

$$\begin{cases} N_{st} = \frac{\sqrt{\Phi_t}}{\sqrt[4]{\Psi_t^3}} \\ D_{st} = \frac{\sqrt[4]{\Psi_t}}{\sqrt{\Phi_t}} \end{cases} \quad (6)$$

165 In particular, solving the first equation of the system for $\sqrt{\Phi_t}$ and inserting
166 it in the second one, Ψ_t is:

$$\Psi_t = \frac{1}{(N_{st} D_{st})^2}. \quad (7)$$

Then, once Ψ_t has been computed, Φ_t is evaluated through one of the two equations of System (6). The corresponding dimensional magnitudes, i.e. flow rate (Q) and head (H), are obtained by the following equations:

$$Q = \Phi \cdot \omega \cdot D^3 \quad (8)$$

$$H = \frac{\Psi \cdot \omega^2 \cdot D^2}{g} \quad (9)$$

167 As reported in Section 1, the proposed prediction model supplies a further in-
168 dication of the mechanical efficiency of PaTs at their BEP. In the literature, some

169 correlations between the mechanical efficiency of a PaT operating in both pump
 170 and turbine modes have already been proposed. Alatorre-Frenk [26] suggested a
 171 direct correlation between mechanical efficiencies in both operating modes, as-
 172 suming η_t equal to η_p minus 0.03. Other authors provided correlations between
 173 two variables, such as Schmiedl [27], that correlate η_t with η_p and N_{st} , while
 174 Grover [28] requires to identify N_{st} from experimental tests.

175 However, a priori knowledge of the N_{st} values needs a model to predict the
 176 BEP in turbine mode or data obtained by experimental campaigns. For instance,
 177 N_{st} could be obtained by means of a correlation that uses non-dimensional pa-
 178 rameters in pump mode at BEP, but its prediction inevitably affects the accuracy
 179 of the mechanical efficiency forecast in turbine mode η_t . In order to find out an
 180 accurate correlation to predict η_t , several combinations of non-dimensional pa-
 181 rameters in pump mode were used. In particular, polynomial equations with two
 182 parameters were studied in order to obtain higher forecast capabilities.

183 Table 2 reports the forecast accuracy, in terms of R^2 -values, achieved by using
 184 second order polynomial equations with different non-dimensional parameters
 185 as independent variables. For sake of conciseness, only the top three results are
 186 reported. Among them, the best correlation was obtained by expressing η_t as a
 187 function of N_{sp} and η_p , achieving an R^2 -value equal to 0.7857.

188 The trend of η_t , which is described by the second order Equation (10), is
 189 shown in Figure 4.

Table 2: R^2 -values obtained by correlating two different non-dimensional parameters

1 st variable	2 nd variable	R^2 -value
N_{sp}	η_p	0.7857
Φ_p	η_p	0.7649
Λ_p	η_p	0.7452

$$\eta_t = 0.7933 \cdot N_{sp} + 0.605 \cdot \eta_p - 0.09246 \cdot N_{sp}^2 - 0.8254 \cdot (N_{sp} \cdot \eta_p) + 0.3936 \cdot \eta_p^2. \quad (10)$$

190 The R^2 -value obtained through Equation (10) is lower than the ones achieved
 191 by the linear Equations (4) and (5) for predicting both specific speed N_s and
 192 specific diameter D_s , respectively. However, since the mechanical efficiency is

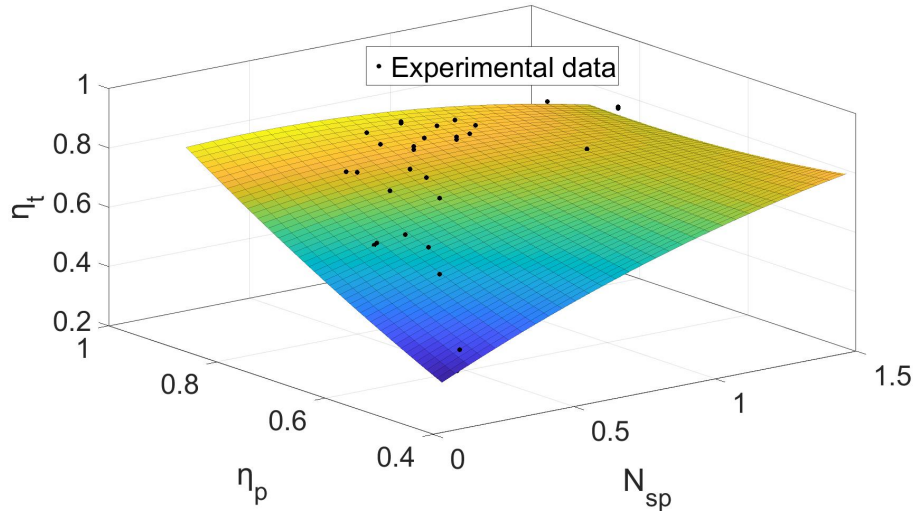


Figure 4: 3D plot of η_t as a function of N_{sp} and η_p

193 linked not only to the operating principle of the machine but also to its specific
 194 design and typology, the result could be considered, either way, satisfactory.

195 Finally, it is worth noticing that an increase in the forecast capability of the
 196 model could be obtained by increasing the number of PaTs involved in the ex-
 197 perimental data-set, as well as widening the range of N_s by adding data of other
 198 PaTs typologies.

199 3. Experimental tests and numerical analysis

200 An experimental apparatus was designed to obtain the operating data of a
 201 centrifugal pump (PaT A) operating in both direct and reverse modes. In addition,
 202 a numerical analysis was performed on the same hydraulic machine. The
 203 comparison between experimental and numerical data of this PaT has been used
 204 to validate the numerical CFD simulations. The same CFD numerical models
 205 have been employed to assess the operating performance of another two PaTs
 206 (PaT B and PaT C), since experimental data on these two machines were not
 207 available. Furthermore, an additional three pumps (PaT D, PaT E and PaT F),
 208 whose data were provided by Brno University of Technology (BUT) and Poly-
 209 technic University of Bari (POLIBA), were used to further assess the prediction
 210 capability of the proposed model.

211 The experimental campaign and the numerical simulations have already been
 212 performed and discussed in detail in a previous work by the authors. Therefore,
 213 for the sake of conciseness, this Section has the aim to briefly describe only the
 214 main equipment that composes the test bench and the main numerical methods
 215 used to perform the CFD simulations. For further details, please refer to [16].

216 The experimental apparatus is constituted by: i) a flow meter, ii) two pres-
 217 sure probes, which are located in proximity to the volute’s openings and iii) the
 218 torque meter that links the shaft of the PaT to the electric motor/brake. It is
 219 worth noticing that the electric generator is constituted by a two pole pairs syn-
 220 chronous motor. A frequency converter was used in the laboratory set-up but,
 221 for the current tests, the frequency was kept at the rated value of 50 Hz . No
 222 additional closed loop controller was used, therefore the rotational speed was
 223 equal to 1450 rpm . The electric power produced by the PaT was then dissipated
 224 using appropriate electric resistors to avoid introducing harmonic frequencies
 225 in the grid that would have affected its reliability and safety. Table 3 lists the
 226 characteristics of the equipment previously mentioned.

Table 3: Technical data of the equipment that constitute the test rig

Measured quantity	Measurement equipment	Range	Accuracy	Signal
Flow rate	Endress+Hauser Promag 50 W	$0.3 - 10\text{ m/s}$	0.5% (0.2% optional)	$4 - 20\text{ mA}$
Pressure	Keller PA33X	$0 - 10\text{ bar}$	0.1% FS Error band ($10 - 40$) °C	$0 - 10\text{ V}$
Torque	Kistler Type 4503A50	$0 - 50\text{ Nm}$	0.1 - 0.2%	$0 - 5\text{ V}$

227 Figure 5 shows the experimental set-up, highlighting the equipment in order
 228 to have a general overview of the used test bench, while Figure 6 displays a
 229 general scheme of the used test bench.

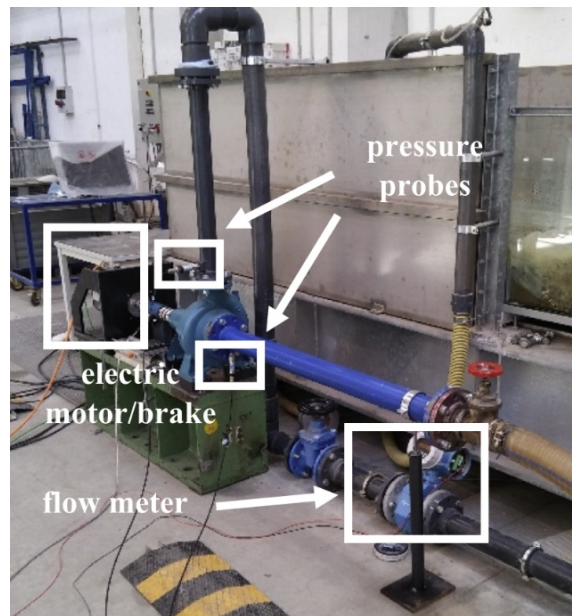


Figure 5: Used test bench [16, 30]

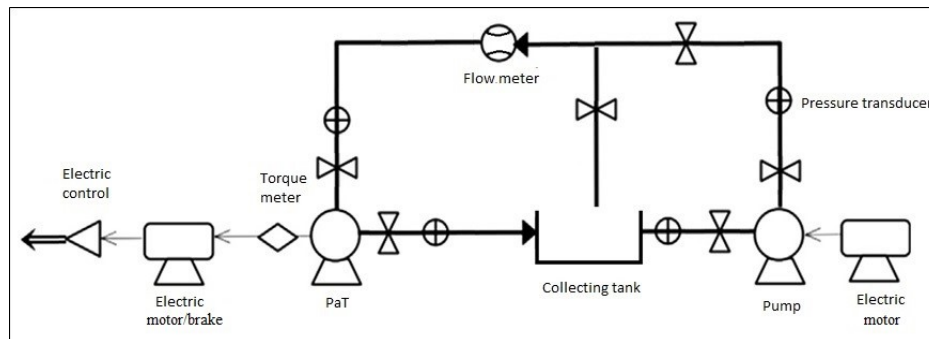


Figure 6: Scheme of the test bench [16, 30]

230 The overall measurement inaccuracy, considering the error propagation, is
 231 0.72% for the hydraulic power, 0.32% for the mechanical power and 0.85% for
 232 the mechanical efficiency [16]. Laboratory tests were performed by keeping the
 233 rotating speed of the PaT constant at 1450 *rpm*, as previously said, and vary-
 234 ing the flow rate exploited by the hydraulic machine with a 3-way valve. This
 235 procedure has been performed for both operating modes of PaT A, allowing a
 236 reconstruction of the entire performance curves, such as characteristic, power

237 and mechanical efficiency curves. Table 4 lists the experimental data of PaT A,
 238 operating at BEP in both pump and turbine modes.

Table 4: Experimental data of PaT A at BEP in both pump and turbine modes

Magnitude	Pump mode	Turbine mode
Flow rate [m^3/s]	0.014	0.021
Head [m]	10.0	15.0
Efficiency [-]	0.76	0.76
Rotating speed [rpm]		1450
Specific Speed [-]	0.57	0.53
Impeller Diameter [m]		0.193
Specific Diameter [-]	5.15	4.66
Number of blades		7
Liquid processed		H_2O ($\rho \approx 1000 \text{ kg}/m^3$)

239 The numerical analysis was performed with the commercial ANSYS® soft-
 240 ware package and, in particular, using the CFX® solver [35] based on the Finite
 241 Volume Method (FVM). The mesh grid independence was ensured by successive
 242 mesh refinements until a maximum difference of 0.7%, in terms of two contigu-
 243 ous results of head, was achieved [16].

244 The experimental data of PaT A, which are reported in Table 4, were used
 245 to validate the accuracy of the numerical results obtained for the same machine.
 246 Considering the values of head and efficiency obtained by the CFD simulations
 247 in both pump and turbine modes, a maximum absolute relative error of 2.00%
 248 was achieved, which represents a very good result for the engineering practice
 249 [16]. After the validation of the simulations, the same numerical CFD models
 250 were used to perform the CFD simulations on 3D CAD geometries of both PaT
 251 B and PaT C.

252 The authors of this work have already validated the CFD simulations of PaT
 253 B and PaT C by means of an analytical model, based on experimental data, which
 254 was described and applied in [16], showing a good forecast capability both at BEP
 255 and in off-design operating conditions ($\pm 40\%$ with respect to BEP) in turbine
 256 mode.

257 Since PaTs belong to the turbomachinery category, an interface between sta-
 258 tionary and rotating domains was created in the definition of the computational

259 fluid domain. In this work, the Frozen Rotor Model (FRM) [35], which is a steady-
 260 state method that allows a reduction in the computational effort using rotating
 261 reference frame, was used. Regarding diffusive and convective terms, both of
 262 them were discretized with High-Resolution schemes [36]. Reynolds Averaged
 263 Navier-Stokes (RANS) equations, coupled with the standard $k - \omega$ two-equation
 264 model, were used for running steady-state simulations of the turbulent flow. For
 265 the near wall-treatment, the automatic wall function was employed, which is a
 266 blending between viscous sublayer and log-law relation. Finally, the normalized
 267 residuals drop, considering all the simulations, was between 10^{-5} and 10^{-10} . As
 268 a result, y^+ values below 30 were obtained along the impeller walls. However,
 269 y^+ values close to 250 – 300 were detected in tip gap regions, which are consid-
 270 ered still reasonable if the global performance of a hydraulic machine has to be
 271 evaluated [37], without focusing the attention on the leakage flow field.

272 To have an overview of the spatial discretization for the simulations of PaTs
 273 A, B and C, the numbers of elements of the mesh in the single fluid domains are
 274 reported in Table 5.

Table 5: Mesh elements of PaTs A, B and C

Geometry	n° of elements of PaT A	n° of elements of PaT B	n° of elements of PaT C
Impeller	1,398,917	743,544	1,514,004
Inlet/Exit pipes	195,342	84,319	107,752
Volute	431,669	277,643	182,814
Total	2,025,928	1,055,506	1,804,670

275 The numerical results obtained in both operating modes of PaTs A, B and C
 276 at BEP are instead shown in Table 6.

Table 6: Numerical data of PaTs A, B and C at their BEPs in both direct and reverse modes

Characteristics	PaT A		PaT B		PaT C	
	Pump mode	Turbine mode	Pump mode	Turbine mode	Pump mode	Turbine mode
Flow rate [m^3/s]	0.014	0.021	0.077	0.109	0.120	0.228
Head [m]	10.20	14.70	21.59	20.80	32.00	70.40
Efficiency [-]	0.75	0.76	0.80	0.79	0.66	0.67
Rotating speed [rpm]		1450		1450		1500
Specific speed [-]	0.57	0.51	0.76	0.93	0.73	0.56
Impeller Diameter [m]		0.193		0.281		0.340
Specific diameter [-]	5.16	4.62	3.86	3.22	4.13	3.65
Number of blades		7		6		10
Liquid processed		H_2O		H_2O		H_2O
		($\rho \approx 1,000 \text{ kg/m}^3$)		($\rho \approx 1,000 \text{ kg/m}^3$)		($\rho \approx 1,000 \text{ kg/m}^3$)

277 Along the same line, the experimental data of PaT D, PaT E and Pat F in both
 278 operating modes are shown in Table 7.

Table 7: Experimental provided data of PaTs D, E and F at their BEPs in both direct and reverse modes

Characteristics	PaT D		PaT E		PaT F	
	Pump mode	Turbine mode	Pump mode	Turbine mode	Pump mode	Turbine mode
Flow rate [m^3/s]	0.032	0.041	0.064	0.093	0.122	0.177
Head [m]	34.70	49.01	26.80	33.40	21.81	34.92
Efficiency [-]	0.79	0.79	0.82	0.80	0.84	0.84
Rotating speed [rpm]		2900		1000		1000
Specific speed [-]	0.69	0.60	0.41	0.41	0.65	0.55
Impeller Diameter [m]		0.174		0.419		0.405
Specific diameter [-]	4.15	4.03	6.66	5.86	4.44	4.15
Number of blades		6		6		7
Liquid processed		H_2O		H_2O		H_2O
		($\rho \approx 1,000 \text{ kg/m}^3$)		($\rho \approx 1,000 \text{ kg/m}^3$)		($\rho \approx 1,000 \text{ kg/m}^3$)

279 4. Results and comments

280 The operating data of the six centrifugal PaTs described in the previous sec-
 281 tion were not involved in the development of the presented model; therefore,
 282 they were used as a validation data-set for validating the proposed BEP predic-
 283 tion model with a fair comparison. BEP values obtained by laboratory tests (PaTs
 284 A, D, E and F) and numerical simulations (PaTs B and C) are also compared with
 285 the forecast values obtained using the models developed by other researchers,

286 such as [26, 27, 28, 25], in order to assess their singular and global prediction
 287 accuracy.

288 Table 8 lists the BEP data of the six centrifugal PaTs and the forecast ones
 289 using the proposed model, while Table 9 shows the comparison between its ac-
 290 curacy and one of the other models available in the literature. The comparison,
 291 which is performed by using the relative percentage error between experimen-
 292 tal/numerical data and the forecast ones at BEP, is also shown in Figure 7 for PaT
 293 A, B and C, and in Figure 8 for PaT D, E and F.

Table 8: Experimental/Numerical vs predicted BEP values for the six PaTs using the presented model

PaT A	Φ	Ψ	η	Λ	N_s	D_s
BEP _{Exp.}	0.0197	0.1713	0.76	0.0026	0.53	4.58
BEP _{Model}	0.0167	0.1565	0.75	0.0020	0.52	4.87
PaT B	Φ	Ψ	η	Λ	N_S	D_S
BEP _{CFD}	0.0324	0.1121	0.79	0.00286	0.93	3.22
BEP _{Model}	0.0303	0.1595	0.77	0.00369	0.69	3.63
PaT C	Φ	Ψ	η	Λ	N_s	D_s
BEP _{CFD}	0.0369	0.24	0.67	0.00594	0.54	3.01
BEP _{Model}	0.0468	0.2358	0.70	0.00773	0.64	3.22
PaT D	Φ	Ψ	η	Λ	N_s	D_s
BEP _{Exp.}	0.0255	0.1722	0.79	0.0042	0.60	4.03
BEP _{Model}	0.0268	0.1693	0.78	0.0045	0.62	3.92
PaT E	Φ	Ψ	η	Λ	N_s	D_s
BEP _{Exp.}	0.0120	0.1702	0.80	0.0021	0.41	5.86
BEP _{Model}	0.0109	0.1852	0.79	0.0020	0.37	6.28
PaT F	Φ	Ψ	η	Λ	N_s	D_s
BEP _{Exp.}	0.0254	0.1899	0.84	0.0044	0.55	4.15
BEP _{Model}	0.0230	0.1636	0.81	0.0038	0.59	4.19

Table 9: Relative percentage errors between experimental/numerical and predicted BEP values

Error(%) PaT A	Φ	Ψ	η	Λ	N_s	D_s
This paper	-15.23	-8.64	-1.32	-23.08	-1.90	+6.33
Alatorre-Frenk [26]	-43.78	+11.01	-3.95	-45.08	-30.67	+36.90
Schmiedl [27]	+10.53	+25.96	+3.65	+32.19	-11.58	+0.77
Grover [28]	+57.69	+78.74	-13.12	+124.33	-	-7.92
Tan et al.[25]	-35.41	-25.52	+6.86	-52.91	+0.24	+15.59
Error(%) PaT B	Φ	Ψ	η	Λ	N_s	D_s
This paper	-6.48	+42.28	-2.53	+29.02	-25.81	+12.73
Alatorre-Frenk [26]	-45.52	+56.43	-2.53	-75.346	-47.23	+51.52
Schmiedl [27]	+5.96	+79.05	+0.69	-43.29	-33.50	-12.37
Grover [28]	+66.33	+177.32	-13.95	+17.81	-	+0.06
Tan et al.[25]	-26.68	+28.44	+3.57	-71.05	-29.03	+24.33
Error(%) PaT C	Φ	Ψ	η	Λ	N_s	D_s
This paper	+26.83	-1.75	+4.48	+30.13	+18.52	+6.98
Alatorre-Frenk [26]	-43.25	-0.40	-5.97	-91.09	-23.12	+30.34
Schmiedl [27]	+16.32	+16.87	+0.04	-77.97	-4.05	-3.59
Grover [28]	+28.72	+31.18	-14.61	-76.64	-	-5.67
Tan et al.[25]	-46.02	-44.24	+1.41	-95.06	+13.85	+17.62
Error(%) PaT D	Φ	Ψ	η	Λ	N_s	D_s
This paper	+5.10	-1.68	-1.27	+7.14	+3.33	-2.73
Alatorre-Frenk [26]	-37.25	+9.52	-3.80	-28.57	-26.67	+29.53
Schmiedl [27]	+22.35	+24.91	+1.27	+59.52	-6.87	-4.22
Grover [28]	+87.84	+89.72	-13.92	+271.43	-	-14.14
Tan et al.[25]	-19.61	-15.97	+3.80	-28.57	+1.67	+6.95
Error(%) PaT E	Φ	Ψ	η	Λ	N_s	D_s
This paper	-9.17	+8.81	-1.25	-4.76	-9.76	+7.17
Alatorre-Frenk [26]	-48.33	+14.57	-1.25	-42.86	-34.15	+44.54
Schmiedl [27]	-0.83	+32.31	+10.00	+28.57	-18.70	+7.85
Grover [28]	+64.17	+115.33	-10.00	+242.86	-	-5.46
Tan et al.[25]	-39.17	-25.03	+13.75	-57.14	-2.44	+19.45
Error(%) PaT F	Φ	Ψ	η	Λ	N_s	D_s
This paper	-9.45	-13.85	-2.99	-13.64	+7.27	+0.96
Alatorre-Frenk [26]	-50.39	-14.43	-3.59	-54.55	-20.00	+36.39
Schmiedl [27]	-5.12	-0.42	+1.80	+2.27	-1.66	+2.41
Grover [28]	+62.99	+67.40	-13.77	+200.00	-	-11.08
Tan et al.[25]	-31.10	-26.65	+5.39	-45.45	+5.45	+11.33

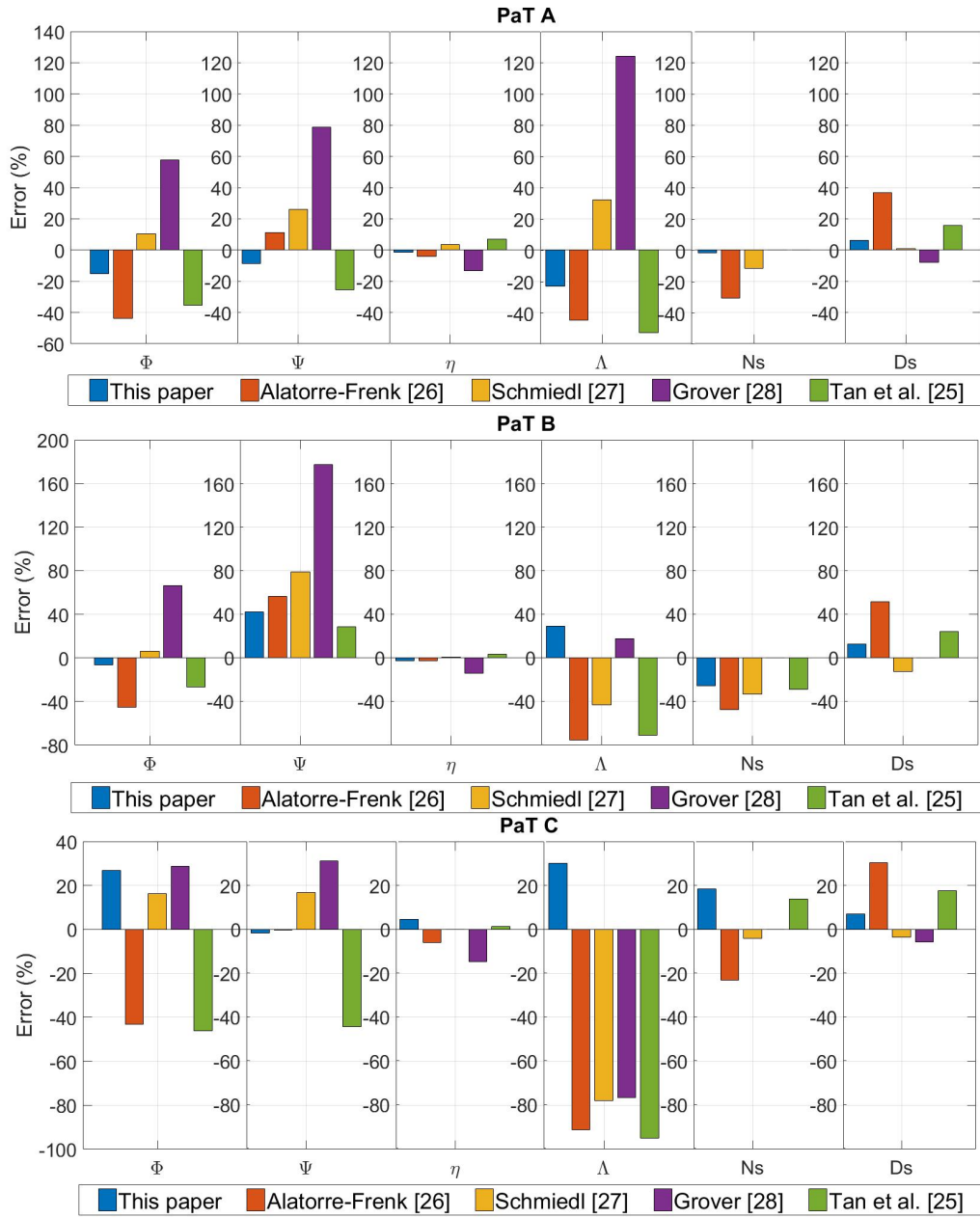


Figure 7: Comparison between the errors obtained by this paper and by another four models available in literature for PaT A (top row), PaT B (middle row) and PaT C (bottom row)

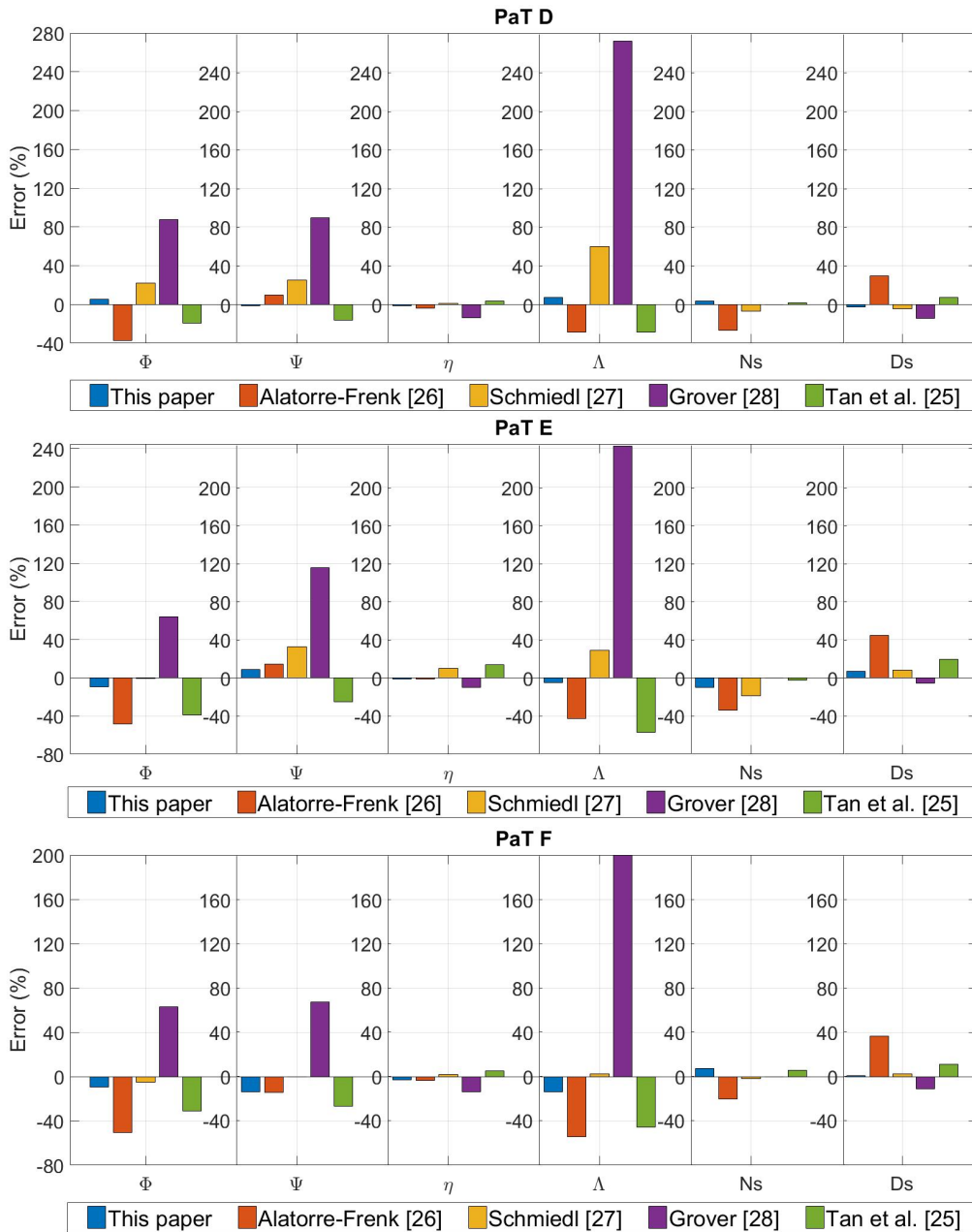


Figure 8: Comparison between the errors obtained by this paper and by another four models available in literature for PaT D (top row), PaT E (middle row) and PaT F (bottom row)

294

Table 8 shows that the values obtained by using the presented model are close

295 to the experimental/numerical ones globally.

296 Furthermore, as highlighted in Table 9, Figures 7 and 8, even if some forecast
 297 values present relatively high differences with respect to the reference ones, they
 298 show a general good prediction capability when compared to other analytical
 299 methodologies available in the literature.

300 In order to compare the accuracy of the considered models globally, the av-
 301 erage error for each method, taking into account the results obtained by all the
 302 six PaTs, is evaluated as:

$$\overline{\text{Error } a} (\%) = \frac{\sum_{k=1}^6 |\text{Error } a_{PaTk} (\%)|}{6} \quad (11)$$

303 where "a" is a generic variable. In Table 10 and Figure 9, the average errors
 304 obtained by each model related to the main operating parameters are reported
 305 and shown. It is worth noticing that both flow rate and head coefficient errors
 306 are higher than the ones related to the mechanical efficiency due to the error
 307 propagation linked to the the developed correlations between specific speeds
 308 and specific diameters of PaTs operating in both pump and turbine modes, re-
 309 spectively.

Table 10: Average errors between experimental/numerical and considered models data

$\overline{\text{Error}} (\%)$	Φ	Ψ	η	Λ	N_s	D_s
This paper	12.04	12.84	2.31	17.96	11.10	6.15
Alatorre-Frenk [26]	44.75	17.73	3.52	56.25	30.31	38.20
Schmiedl [27]	10.19	29.92	2.91	40.64	12.73	5.20
Grover [28]	61.29	93.28	13.23	155.51	—	7.39
Tan et al.[25]	33.00	27.64	5.80	58.36	8.78	15.88

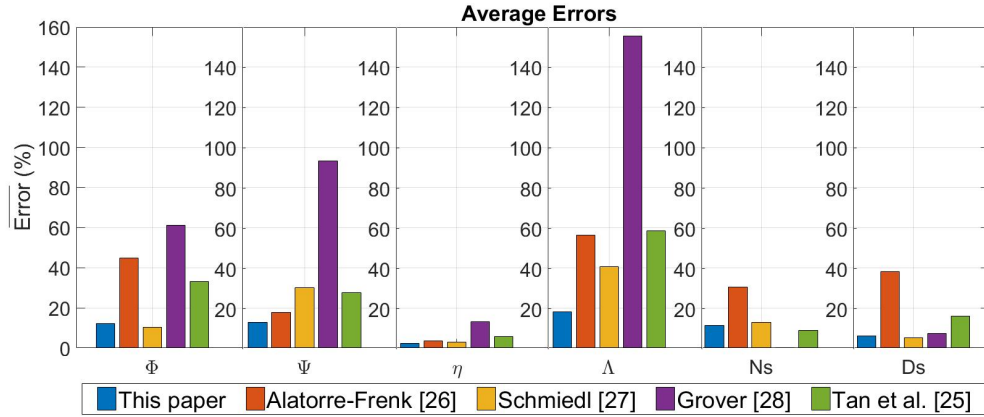


Figure 9: Comparison between the average errors obtained by this paper and selected models available in the literature

310 Considering the outcomes of this analysis (see Table 9, Figures 7 and 8, Table
 311 10 and Figure 9), a detailed analysis of the prediction capability related to the
 312 model described in this work is discussed. Moreover, a comparison between the
 313 results obtained by this model and the ones of the four models available in the
 314 literature, chosen as terms of comparison, is performed.

315 In particular, it is possible to highlight the following aspects:

- 316 • Flow coefficient (Φ): the model of Schmiedl [27] obtained the best result,
 317 reaching a maximum error of 22.35% for PaT D and an average one of
 318 10.19%. The second best model is the presented one that had a maximum
 319 error of 26.83% for PaT C, while the average error was equal to 12.04%,
 320 being very close to the one achieved by Schmiedl [27]. Regarding the other
 321 models, they achieved both maximum and average errors higher than 33%.
- 322 • Head coefficient (Ψ): the presented model is the most accurate, showing
 323 an average error of 12.84%. It follows the model of Alatorre-Frenk [26]
 324 with an average error of 17.73%, whereas the average errors obtained by
 325 the other models were higher than 27%.
- 326 • Mechanical efficiency (η): the presented model obtained the best results
 327 globally, achieving a maximum error equal to 4.48% for PaT B and an
 328 average one of 2.31%. Along the same line, the model of Schmiedl [27],
 329 together with the ones of Alatorre-Frenk [26] and Tan et al. [25], got in-
 330 dicatively the same results, even though the maximum and average errors

331 were slightly higher than the presented model. On the other hand, Grover
332 [28] obtained the worst results, showing errors higher than 10% for each
333 PaT and, consequently, an average error equal to 13.23%.

334 • Power coefficient (Λ): the presented model gained the best results globally,
335 reaching a maximum error of 30.13% for PaT C and an average error equal
336 to 17.96%. All the other models obtained maximum errors higher than
337 77%. Regarding the average errors, the other models showed values higher
338 than 40%. The reason for these results the fact that the power coefficient
339 is a derived variable, which is evaluated as $\Lambda = \eta \cdot \Phi \cdot \Psi$; thus, the error
340 propagation contributes to increase the difference between the reference
341 data and the predicted ones.

342 • Specific speed (N_s): the model of [28] has no error since it is based on a
343 priori knowledge of this parameter in turbine mode. On the other hand,
344 the model of Tan et al. [25], the presented model and the one of Schmiedl
345 [27] gave the best results, showing average errors around 10%. The model
346 of [26] reached a maximum error of -47.23% for PaT B and an average
347 error of about 30%.

348 • Specific diameter (D_s): in this case, Schmiedl [27] obtained the best result
349 with an average error of 5.20%. It follows the presented model and the one
350 of Grover [28] that obtained good results globally. In fact, even if maximum
351 errors close to $\pm 13\%$ were achieved by both models, the average errors
352 were equal to 6.15% and 7.39%, respectively. Regarding the other models,
353 both maximum and average errors were higher than 15%.

354 Considering the above-mentioned evaluations, it can be stated that the accu-
355 racy of the proposed model, as well as of those available in literature, is affected
356 by the non-dimensional parameters used for their development. Nevertheless,
357 the accuracy of the BEP prediction obtained through the presented model was
358 sometimes better or, at least comparable to the best results obtained by the other
359 models. Furthermore, examining the entries of Table 9, it is important to high-
360 light that the presented model shows average errors that are always lower than
361 17.96%, whereas the other models showed a broader range of errors, even though
362 sometimes they resulted in more accurate predictions of single non-dimensional
363 parameters. Certainly, an increase of the experimental data-set on PaTs perfor-
364 mance, as well as widening the typology of tested machines, would lead to a
365 higher reliability of the proposed model and, subsequently, to predicted values
366 closer to the real ones.

367 5. Conclusions

368 In this paper, a model used to predict BEP values of PaTs was developed by
369 analysing and rearranging the experimental data collected by laboratory tests
370 on 59 PaTs. This goal was achieved by correlating the specific speed (N_s) and
371 the specific diameter (D_s) in pump mode with the ones in turbine mode. More-
372 over, a novel approach regarding the prediction of the mechanical efficiency (η)
373 at BEP in turbine mode was proposed in order to supply a complete definition
374 of the PaT performance. The comparison between experimental/numerical and
375 forecast BEP values, taking into account six different centrifugal PaTs that were
376 not used in the development of the presented model, has shown a good gen-
377 eral agreement. The proposed model was subsequently compared to other four
378 models chosen from the literature. This analysis showed an improvement in the
379 prediction accuracy in terms of obtained maximum and average errors for some
380 of the non-dimensional variables involved in the study of PaTs. Furthermore, the
381 presented model showed a very narrow range of errors with respect to the other
382 investigated ones. A further improvement in the forecasting accuracy would be
383 possible by increasing the number of experimental data, as well as by widening
384 the typology of PaTs used to develop the presented model.

385 Acknowledgements

386 This work has been carried out within the Research project “AI-ALPEN”,
387 CUP: B26J16000300003 funded by the Autonomous Province of Bozen/Bolzano
388 - Italy for University Research-2014.

389 The EFRE-FESR project “TURB_HYDRO, Hydrokinetic turbines, optimiza-
390 tion for sustainable production” (ERDF 2018-2021, CUP: I56C18000040009) sup-
391 port is also acknowledged.

392 In addition, the authors would also like to thank the Brno University of Tech-
393 nology (BUT) for providing all the information related to PaT D and PaT F, as
394 well as the Polytechnic University of Bari (POLIBA) that supplied the same in-
395 formation for PaT E.

396 References

- 397 [1] C.-S. Yi, J.-H. Lee, M.-P. Shim, Site location analysis for small hydropower
398 using geo-spatial information system, *Renewable Energy* 35 (2010) 852–861.

- 399 [2] W. Yunna, C. Quanzhi, The demonstration of additionality in small-scale
400 hydropower CDM project, *Renewable Energy* 36 (2011) 2663–2666.
- 401 [3] H. Borhanazad, S. Mekhilef, R. Saidur, G. Boroumandjazi, Potential appli-
402 cation of renewable energy for rural electrification in Malaysia, *Renewable*
403 *Energy* 59 (2013) 210–219.
- 404 [4] T. Lydon, P. Coughlan, A. McNabola, Pressure management and energy re-
405 covery in water distribution networks: Development of design and selec-
406 tion methodologies using three pump-as-turbine case studies, *Renewable*
407 *Energy* 114 (2017) 1038–1050.
- 408 [5] M. Kramer, K. Terheiden, S. Wieprecht, Pumps as turbines for efficient en-
409 ergy recovery in water supply networks, *Renewable Energy* 122 (2018) 17–
410 25.
- 411 [6] M. Renzi, P. Rudolf, D. Štefan, A. Nigro, M. Rossi, Installation of an axial
412 Pump-as-Turbine (PAT) in a wastewater sewer of an oil refinery: a case
413 study, *Applied Energy* 250 (2019) 665–676.
- 414 [7] I. Butera, R. Balestra, Estimation of the hydropower potential of irrigation
415 networks, *Renewable and Sustainable Energy Reviews* 48 (2015) 140–151.
- 416 [8] M. Pérez-Sánchez, F.-J. Sánchez-Romero, P.-A. López-Jiménez, H.-M.
417 Ramos, PATs selection towards sustainability in irrigation networks: Simu-
418 lated annealing as a water management tool, *Renewable Energy* 116 (2018)
419 234–249.
- 420 [9] F. Pugliese, F. D. Paola, N. Fontana, M. Giugni, G. Marini, Experimental
421 characterization of two Pump as Turbine for hydropower generation, *Re-
422 newable Energy* 99 (2016) 180–187.
- 423 [10] J. Delgado, J. P. Ferreira, D. I. C. Covas, F. Avellan, Variable speed opera-
424 tion of centrifugal pumps running as turbines. Experimental investigation,
425 *Renewable Energy* 142 (2019) 437–450.
- 426 [11] S.-V. Jain, R.-N. Patel, Investigations on pump running in turbine mode: A
427 review of the state-of-the-art, *Renewable and Sustainable Energy Reviews*
428 30 (2014) 841–868.

- 429 [12] M. Binama, W.-T. Su, X.-B. Li, F.-C. Li, X.-Z. Wei, S. An, Investigations on
430 pump as turbine (PAT) technical aspects for micro hydropower schemes:
431 A state-of-the-art review, *Renewable and Sustainable Energy Reviews* 79
432 (2017) 148–179.
- 433 [13] S. Huang, G. Qiu, X. Su, J. Chen, W. Zou, Performance prediction of a cen-
434 trifugal pump as turbine using rotor-volute matching principle, *Renewable*
435 *Energy* 108 (2017) 64–71.
- 436 [14] J. Delgado, L. Andolfatto, D.-I.-C. Covas, F. Avellan, Hill chart modelling
437 using the hermite polynomial chaos expansion for the performance predic-
438 tion of pumps running as turbines, *Energy Conversion and Management*
439 187 (2019) 578–592.
- 440 [15] D. Novara, A. McNabola, A model for the extrapolation of the characteristic
441 curves of Pumps as Turbines from a datum Best Efficiency Point, *Energy*
442 *Conversion and Management* 174 (2018) 1–7.
- 443 [16] M. Rossi, A. Nigro, M. Renzi, Experimental and numerical assessment of a
444 methodology for performance prediction of Pump-as-Turbine (PAT) oper-
445 ating in off-design conditions, *Applied Energy* 248 (2019) 555–566.
- 446 [17] S. Derakhshan, A. Nourbakhsh, Theoretical, numerical and experimental
447 investigation of centrifugal pumps in reverse operation, *Experimental Ther-
448 mal and Fluid Science* 32 (2008) 1620–1627.
- 449 [18] P. Singh, F. Nestmann, An optimization routine on a prediction and selec-
450 tion model for the turbine operation of centrifugal pumps, *Experimental*
451 *Thermal and Fluid Science* 34 (2010) 152–164.
- 452 [19] S.-S. Yang, F.-Y. Kong, W.-M. Jiang, X.-Y. Qu, Effects of impeller trimming
453 influencing pump as turbine, *Computer Fluids* 67 (2012) 72–78.
- 454 [20] S.-S. Yang, S. Derakhshan, F.-Y. Kong, Theoretical, numerical and experi-
455 mental prediction of pump as turbine performance, *Renewable Energy* 48
456 (2012) 507–513.
- 457 [21] A. Bozorgi, E. Javidpour, A. Riasi, A. Nourbakhsh, Numerical and experi-
458 mental study of using axial pump as turbine in Pico hydropower plants,
459 *Renewable Energy* 53 (2013) 258–264.

- 460 [22] D.-R. Giosio, A.-D. Henderson, J.-M. Walker, P.-A. Brandner, J.-E. Sargison,
461 P. Gautam, Design and performance evaluation of a pump-as-turbine micro-
462 hydro test facility with incorporated inlet flow control, *Renewable Energy*
463 78 (2015) 1–6.
- 464 [23] S.-V. Jain, A. Swarnkar, K.-H. Motwani, R.-N. Patel, Effects of impeller di-
465 ameter and rotational speed on performance of pump running in turbine
466 mode, *Energy Conversion and Management* 89 (2015) 808–824.
- 467 [24] S. Barbarelli, M. Amelio, G. Florio, Predictive model estimating the perfor-
468 mances of centrifugal pumps used as turbines, *Energy* 107 (2016) 103–121.
- 469 [25] X. Tan, A. Engeda, Performance of centrifugal pumps running in reverse
470 as turbine: Part II- systematic specific speed and specific diameter based
471 performance prediction, *Renewable Energy* 99 (2016) 188–197.
- 472 [26] C. Alatorre-Frenk, Cost minimisation in micro-hydro systems using Pump
473 as Turbine, Ph.D. thesis, University of Warwick (1994).
- 474 [27] E. Schmiedl, *Serien-Kreiselpumpen im Turbinenbetrieb*, Pumpentagung
475 Karlsruhe (1988) 357 pp. (in German).
- 476 [28] K.M Grover, *Conversion of pumps to turbines*, GSA Inter Corp., Katonah,
477 New York, USA.
- 478 [29] S. Barbarelli, M. Amelio, G. Florio, Experimental activity at test rig validat-
479 ing correlations to select pumps running as turbines in microhydro plants,
480 *Energy Conversion and Management* 149 (2017) 781–797.
- 481 [30] M. Rossi, M. Renzi, A general methodology for performance prediction of
482 Pump-as-Turbine using Artificial Neural Networks, *Renewable Energy* 128
483 (2018) 265–274.
- 484 [31] M. Venturini, L. Manservigi, S. Alvisi, S. Simani, Development of a physics-
485 based model to predict the performance of Pumps as Turbines, *Applied En-
486 ergy* 231 (2018) 343–354.
- 487 [32] A.-J. Stepanoff, *Centrifugal and Axial Flow Pumps*, John Wiley, New York,
488 NY, USA.
- 489 [33] K. Sharma, *Small Hydroelectric Project-Use of Centrifugal Pumps as Tur-
490 bines*, Technical Report, Kirloskar Electric Co.: Bangalore, India.

- 491 [34] M. Stefanizzi, M. Torresi, B. Fortunato, S. M. Camporeale, Experimental in-
492 vestigation and performance prediction modeling of a single stage centrifu-
493 gal pump operating as turbine, *Energy Procedia* 126 (2017) 589–596.
- 494 [35] ANSYS-CFX, Fluid dynamic software, ANSYS Inc. <https://www.ansys.com>,
495 last accessed on the 16th of July 2019.
- 496 [36] T. J. Barth, D. C. Jespersen, The design and application of upwind schemes
497 on unstructured meshes, *AIAA Paper* 89-0366 1989.
- 498 [37] Y. Liu, L. Tan, Tip clearance on pressure fluctuation intensity and vortex
499 characteristics of a mixed flow pump as turbine at pump mode, *Renewable*
500 *Energy* 129 (2018) 606–615.